A Compact UWB Bandpass Filter With WLAN Rejection Using a Slot Ring Resonator

Shen, Ming; Tong, Tian; Jensen, Ole Kiel; Mikkelsen, Jan H.; Larsen, Torben

Published in:
Microwave & Optical Technology Letters

DOI (link to publication from Publisher):
10.1002/mop.25381

Publication date:
2010

Document Version
Early version, also known as pre-print

previous simulation results. The first and the last bits in the dropped channel have slightly higher power level than others due to the pattern effect in a SOA. The measured signal-to-noise ratios (SNR) are 11.4 dB and 10.2 dB for dropped channel and remained channel, respectively. Due to the limit of experimental conditions, the adding function was not demonstrated in this experiment. However, it could be found that the vacant time slots on the remained channel are clean enough for adding a new channel by using a passive coupler and an appropriate time delay.

Further simulations (not shown) suggest that the proposed OADM function could operate at higher bit rates, which is depended on the performance of the SOA, especially the carrier recovery time. On the whole, FWM will not limit the working speed of the module, since it is dominated by ultra-fast carrier dynamics. But the slow carrier recovery time is an obstacle in the XGM process. Fortunately, several operational parameters can be adjusted to reduce the carrier recovery time, such as increasing the injection current, increasing the optical power or using assist light. Though fine-tuning these parameters, this module is able to work at significantly higher bit rates.

4. CONCLUSIONS

We have proposed a simple and compact OADM configuration by using only a single SOA. FWM and XGM effects in SOA are employed to generate dropping and clearing channel. Good performance is shown by both simulation and experiment at 10 Gbit/s. In addition, the module can be scaled to higher bit rates by utilizing better device or optimizing some parameters.

ACKNOWLEDGMENTS

This work was supported in part by the Funds for International Cooperation Foundation of Guizhou Province of China under Grant No. (2009) 700102, special fund for technology and education talents of Guizhou Province of China under Grant No. (2009) 98, and the Funds for import of talents of Guizhou university Grant No. (2008) 010.

REFERENCES

1. C. Schubert, C. Schmidt, S. Ferber, R. Ludwig, and H.G. Weber, Error-free all-optical add-drop multiplexing at 160 Gbit/s, Electron Lett 39 (2003), 1074–1076.
2. S. Diez, R. Ludwig, and H.G. Weber, Gain-transparent SOA-switch for high-bit rate OTDM add/drop multiplexing, IEEE Photon Technol Lett 11 (1999), 60–62.
3. A.M. de Melo, S. Randel, and K. Petermann, Mach-Zehnder interferometer-based high-speed OTDM add-drop multiplexing, J Lightwave Technol 25 (2007), 1017–1026.
4. J. Li, B.-E. Olsson, M. Karlsson, and P.A. Andrekson, OTDM add-drop multiplexer based on XPM-induced wavelength shifting in highly nonlinear fiber, J Lightwave Technol 23 (2005), 2654–2661.
5. E.J.M. Verdurmen, Y. Zhao, E. Tangdiongga, J.P. Turkiewicz, et al., Error-free all-optical add-drop multiplexing using HNLF in a NOLM at 160 Gbit/s, Electron Lett 41 (2005), 349–350.
6. P.-M. Gong, J.-T. Hsieh, S.-L. Lee, and J. Wu, Theoretical analysis of wavelength conversion based on four-wave mixing in light-holding SOAs, IEEE J Quantum Electron 40 (2004), 31–40.
7. N.C. Kothari and D.J. Blumenthal, Influence of gain saturation, gain asymmetry and pump/probe depletion on wavelength conversion efficiency of FWM in semiconductor optical amplifiers, IEEE J Quantum Electron 32 (1996), 1810–1816.

A COMPACT UWB BANDPASS FILTER WITH WLAN REJECTION USING A SLOT RING RESONATOR

Ming Shen, Tian Tong, Ole K. Jensen, Jan H. Mikkelsen, and Torben Larsen
Technology Platforms Section, Department of Electronic Systems, Aalborg University, Denmark; Corresponding author: mish@es.aau.dk

Received 27 November 2009

ABSTRACT: *This article presents a novel ultra-wideband bandpass filter with controllable notched bands, compact size, and relaxed fabrication requirements. Its implementation is based on a rectangular slot ring resonator with an embedded S-shaped slotline. The behavior of the rectangular slot ring resonator is characterized and subsequently adopted to build the wide passband. The notched band necessary for rejecting wireless local-area network (WLAN) signals is implemented by the S-shaped slotline. A prototype filter is implemented based on the proposed structure and good agreement is found between simulations and measurements.* © 2010 Wiley Periodicals, Inc. Microwave Opt Technol Lett 52: 1980–1984, 2010; Published online in Wiley InterScience (www.interscience.wiley.com). DOI 10.1002/mop.25381

Key words: *ultra-wideband; bandpass filter; notched-band; slot line; stopband attenuation*

1. INTRODUCTION

In 2002, the Federal Communication Committee (FCC) authorized the unlicensed use of the ultra-wideband (UWB) frequency band from 3.1 to 10.6 GHz for indoor and hand-held systems [1]. Since then, considerable effort has been put into the development of devices suitable for UWB applications [2]. As one of the essential components, UWB bandpass filters (BPF) have attracted significant research interest and various approaches to the design of UWB BPFs have been proposed [3–9]. Based on the fact that the WLAN signals (MMAC HiSWANa: 4.9–5.0 GHz, 5.15–5.25 GHz; ETSI HiperLAN2: 5.15–5.35 GHz, 5.47–5.725 GHz; IEEE 802.11a: 5.15–5.35 GHz, 5.725–5.825 GHz) are located within the UWB frequency band, as shown in Figure 1, UWB systems should expect interferences originating from any one of these WLAN signal bands [2]. To reduce WLAN related interference problems one option is to introduce a stop band in the UWB BPF's response at corresponding frequencies. It could be either a 5–6 GHz stop band for the rejection of all the WLAN bands or a narrow stop band to reject one of the sub bands. UWB bandpass filters following this approach have previously been reported; In one case, a filter based on five short-circuited stubs has been proposed, and embedded open-circuited stubs were used to introduce a notched band [4]. Another filter combines a conventional bandpass characteristic and negative permittivity metamaterial to establish an UWB response and a notch [5]. However, these designs have comparatively large sizes. A compact filter using trilayer structures has the advantage of miniaturized size [6], but it is unsuitable for conventional double layer PCBs. Using a modified multiple mode resonator fed by interdigital coupled lines, an UWB BPF has been built, and a notch band was created by extending and folding one of the two arms in the coupled-line section [7]. A filter based on stubloaded modified stepped impedance resonator and two identical interdigital feed-lines has also been proposed [8]. However, usually narrow strip/slot widths are preferred in the interdigital coupled lines used in these designs (min. gap width of 0.05 mm in [7]), which require tight control of fabrication tolerances.

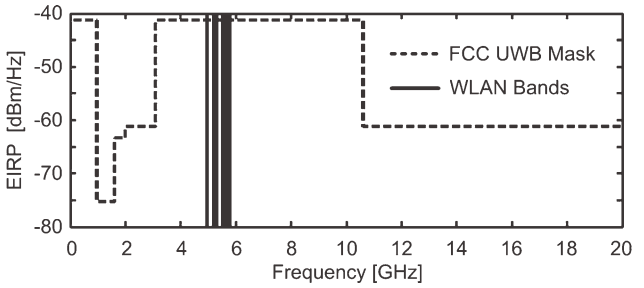

Figure 1 The FCC UWB EIRP mask, and the WLAN bands of different standards

Moreover, although upper stop band (>10.6 GHz) attenuation is important for upper band interference and noise suppression, only few UWB BPFs with notched band and satisfactory upper stop band performance have been reported [7, 9].

This article proposes a novel ultra-wideband bandpass filter that offers compact size, controllable notched bands, and relaxed fabrication requirements. The topology is based on a rectangular slot ring resonator with an S-shaped slotline. In this study, the multimode resonant behavior of the rectangular slot ring is adopted to achieve the ultra-wide passband. The notched band for rejecting WLAN signals is implemented by embedding the S-shaped slotline, while maintaining the small circuit size of 7.8 × 9.4 mm^2. The S-shaped slotline plays a role of a half wavelength resonator, so that a transmission zero can be introduced at the resonant frequency. It is also shown that an upper stopband attenuation of 28 dB can be easily achieved by connecting two low-pass filters (LPF) at both ends of the proposed UWB BPF. A prototype filter is fabricated to verify the design. Simulated and measured results are shown and a comparison with previous work is provided.

2. DESIGN OF THE UWB BPF WITH A NOTCHED BAND

Figure 2(a) shows the proposed rectangular slot ring resonator for the implementation of UWB BPFs with notched bands. It consists of two 50 Ω microstrip feed lines with open stubs (solid lines) on one metal layer of a two-metal-layer substrate, and a rectangular slot ring resonator with an embedded S-shaped slotline (white strips) etched on the other metal layer (shaded area). To clearly explain the principles of this coupling structure, the multimode resonant behavior of the original rectangular slot ring resonator without the S-shaped slotline is studied first. The study is conducted by simulation using the Agilent ADS Momentum simulator with the substrate RT/Duriod 6010 having a relative dielectric constant of $\varepsilon_r = 10.2$, a loss tangent of tan $\delta = 0.0023$ and a thickness of $t = 0.635$ mm.

The original resonator is shown in the embedded figure in Figure 2(b). The equivalent circuit of the original resonator is shown in Figure 2(c), where Z_{0s} and θ_s are the characteristic impedance and half of the electrical length of the slot ring, respectively. Z_{0mo} and θ_{mo} are the characteristic impedance and electrical length of the microstrip open stub, respectively. C_{oc} represents the parasitic capacitance at the end of the open stub, and N is the turns ratio of the transformer modeling the coupling between the microstrip and the slotline. The width of the slotline is set to 0.9 mm to have a characteristic impedance of around 100 Ω for impedance matching, and the width of the open stubs is set relatively wider, to 1.8 mm, for bandwidth improvement [10]. L_1 and L_2 are set to 6.9 and 8.5 mm, respectively. They are related to the resonant frequencies of the resonator [11], which can be determined by

$$2(L_1 + L_2) = n\lambda_s, \tag{1}$$

where λ_s is the slotline wavelength, and n is the mode number. Using Eq. (1), the first three resonant frequencies can be calculated to 4, 8, and 12 GHz for this design. The simulated S_{21}-magnitudes of the resonator for three different values of L_3 are shown in Figure 2(b). The first three resonant modes can be clearly seen at 4.3, 8, and 11.7 GHz when $L_3 = 0.1$ mm, which is in good agreement with Eq. (1). As L_3 increases to 2.9 mm (around one-quarter of the microstrip wavelength at 6.85 GHz),

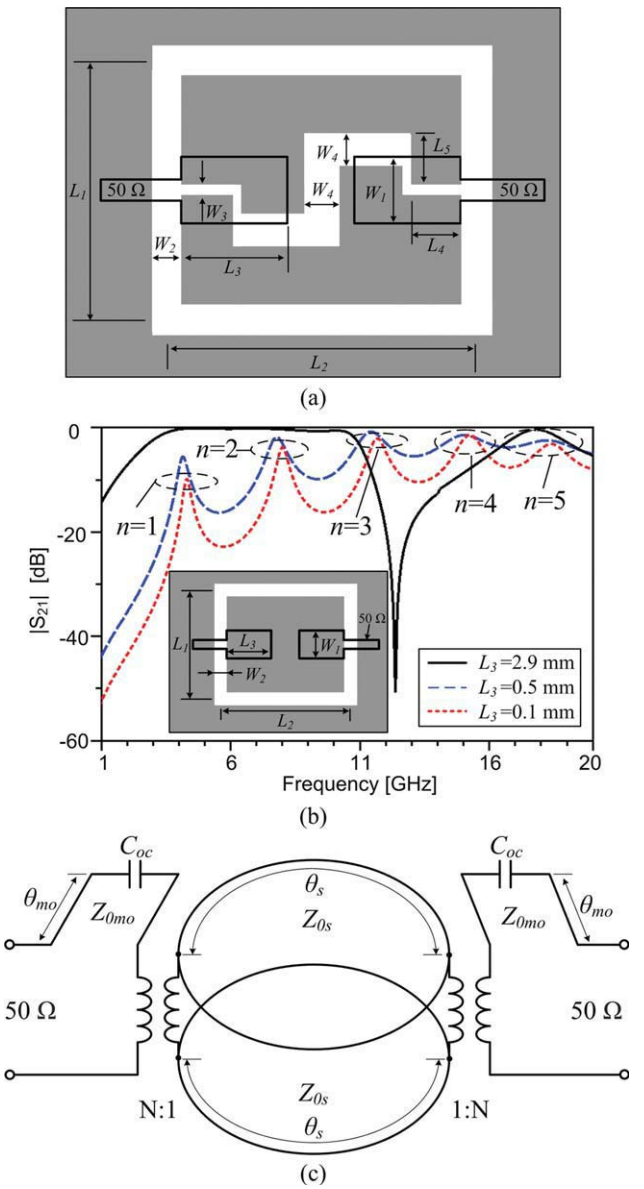

Figure 2 (a) Schematic of the proposed rectangular slot ring resonator, (b) simulated S21-magnitudes versus frequency of the resonator without S-shaped slotline, and (c) the equivalent circuit for the resonator without S-shaped slotline. The parameters for this figure are: $L_1 = 6.9$ mm, $L_2 = 8.5$ mm, $W_1 = 1.8$ mm, $W_2 = 0.9$ mm and varied L_3. [Color figure can be viewed in the online issue, which is available at www.interscience.wiley.com]

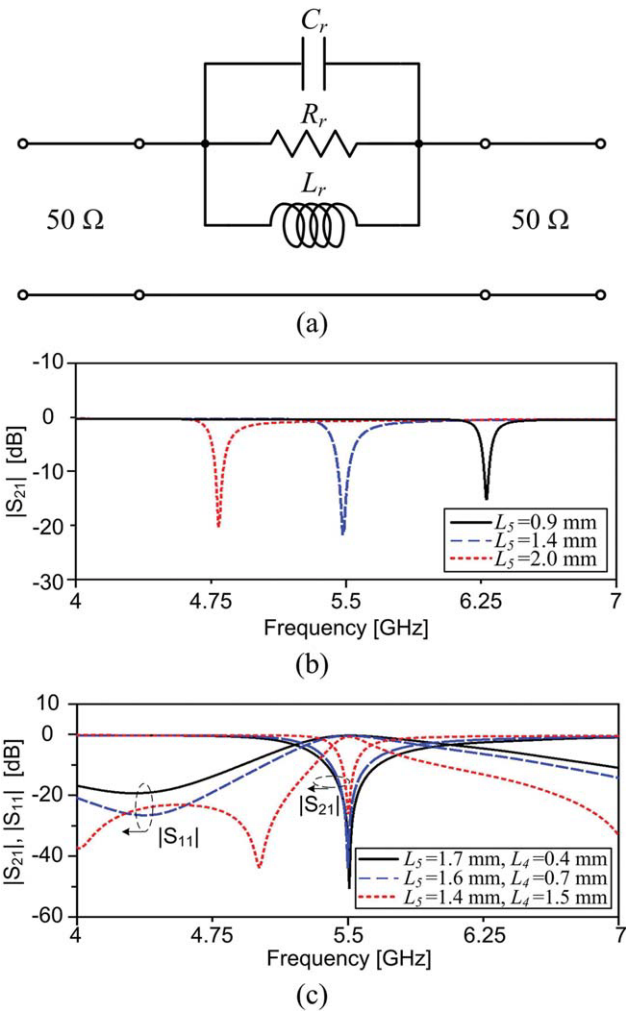

Figure 3 (a) The equivalent circuit for the proposed resonator in the UWB passband, (b) simulated rejection band versus frequency with varied L_5 (L_4 = 1.5 mm) and (c) simulated rejection bandwidth versus frequency with varied L_5 and L_4. The parameters for this figure are: W_1 = 1.8 mm, W_2 = 0.9 mm, W_3 = 0.3 mm, W_4 = 1 mm, L_1 = 6.9 mm, L_2 = 8.5 mm, L_3 = 2.9 mm. [Color figure can be viewed in the online issue, which is available at www.interscience.wiley.com]

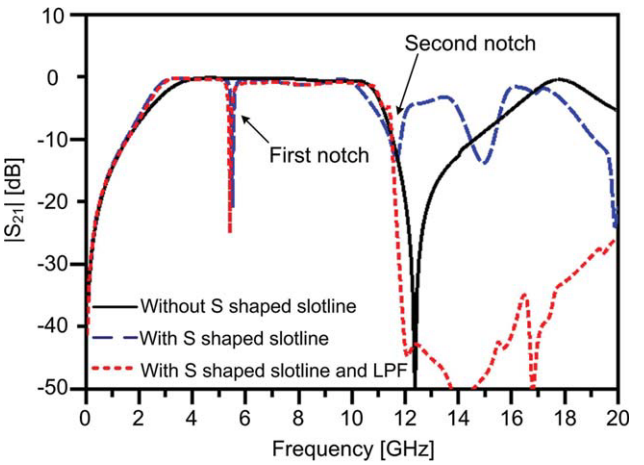

Figure 4 Simulated S21-magnitudes versus frequency of the UWB BPF without the S shaped slotline (without notch), with the S shaped slotline (with notch) and with the S shaped slotline and LPFs. [Color figure can be viewed in the online issue, which is available at www.interscience.wiley.com]

the microstrip open stub can be approximated as a short circuit with neglectable end effects, and the turns ratio N is close to 1. As a result the significance of the resonances is reduced, and a −3-dB ultra-wide passband from 2.8 to 10.9 GHz is achieved.

An extra slotline is further integrated into the slot ring resonator as shown in Figure 2(a) to introduce a notch into the pass band of the UWB BPF. The extra slotline is implemented as an S shape for easily embedding into the original circuit, while maintaining the original circuit size. The S-shaped slot line plays a role of a half wavelength resonator, and it introduces transmission zeros at the resonant frequencies. A parallel resonant circuit as shown in Figure 3(a) is used to model the behavior of the circuit including the S-shaped slotline by simplifying the original microstrip fed slot ring resonator to a 50 Ω transmission line within the UWB pass band. In the circuit, L_r, C_r, and R_r can be extracted from simulations [12]. By modifying the structural parameters of the S-shaped slotline, the location and bandwidth of the notch can be controlled, which can be modeled by varying L_r, C_r, and R_r. Figure 3(b) shows the simulated S_{21}-magnitudes of the proposed structure for a fixed L_4 =

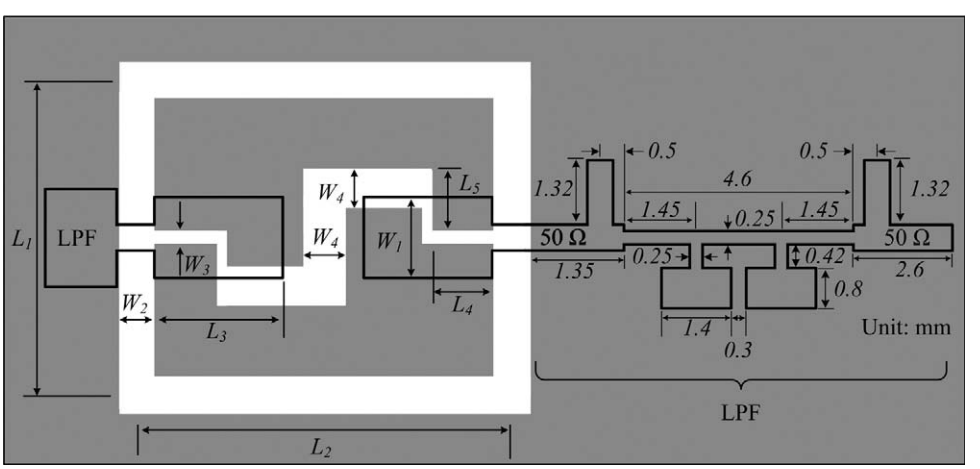

Figure 5 Schematic of the proposed UWB BPF (W_1 = 1.8 mm, W_2 = 0.9 mm, W_3 = 0.3 mm, W_4 = 1.0 mm, L_1 = 6.9 mm, L_2 = 8.5 mm, L_3 = 2.9 mm, L_4 = 1.45 mm, L_5 = 1.4 mm). Only one of the LPFs is shown in details.

1.5 mm and three different values of L_5. It can be seen that the notched band is moved to lower frequencies when the S-shaped slotline is extended by increasing L_5. Simulated S_{21}-magnitudes with varied L_4 and L_5 are shown in Figure 3(c). It can be seen that the −3-dB notched bandwidth can be adjusted from 250 MHz (L_5 = 1.4 mm, L_4 = 1.5 mm) to 1 GHz (L_5 = 1.7 mm, L_4 = 0.4 mm) by modifying L_5 and L_4. This is mainly due to the varying of the capacitance C_r by changing the distance between the bended slot lines. By doing so, the notched band can be adjusted to reject interfering signals of one (for example 5.15–5.35 GHz) or all WLAN bands mentioned in section 1. In this study, L_4 and L_5 are set as 1.45 and 1.4 mm, respectively, to build a notched band at around the central frequency of 4.9–5.83 GHz, i.e., 5.365 GHz as a demonstration. To avoid the undesired impact of the second notch at 10.73 GHz on the UWB pass band, stepped slotlines with width of 0.3 (W_3) and 1 mm (W_4) are used to move the second notch to 11.7 GHz (see Fig. 4). The simulated S_{21}-magnitudes of the UWB BPF with and without notched band are shown in Figure 4.

From Figure 4 it is apparent that the UWB BPF shows limited attenuation in the upper stopband. To show that this drawback can be easily eliminated, two identical low-pass filters based on capacitively loaded transmission lines are connected at two ends of the UWB BPF to improve the upper stopband attenuation. The complete layout of the designed UWB BPF is shown in Figure 5. The simulated S_{21}-magnitude of the UWB BPF with upper stop band improvement is shown in Figure 4. It can be seen that the upper stop band attenuation is drastically improved while the desired UWB BPF response is maintained.

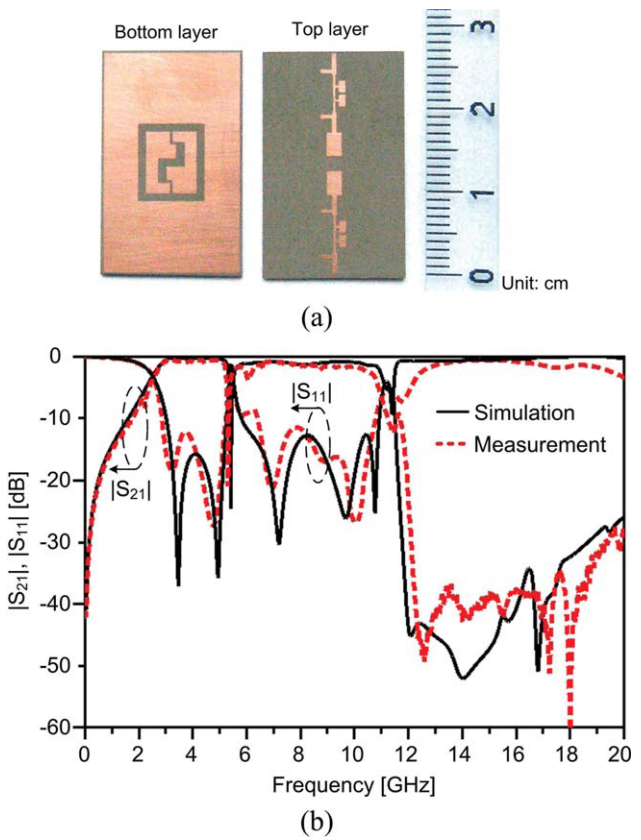

Figure 6 (a) Fabricated UWB BPF, and (b) simulated and measured magnitudes of S-parameters versus frequency of the UWB BPF with a notched band. [Color figure can be viewed in the online issue, which is available at www.interscience.wiley.com]

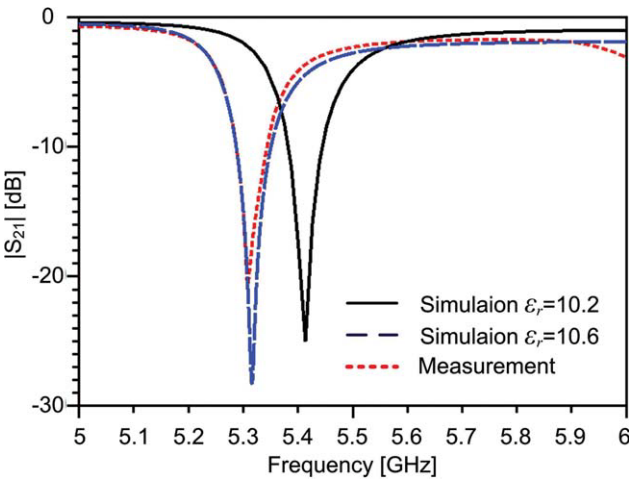

Figure 7 Simulated S21-magnitudes with two different dielectric constants, and the measured S21-magnitudes versus frequency. [Color figure can be viewed in the online issue, which is available at www.interscience.wiley.com]

3. EXPERIMENTS AND RESULTS

The UWB BPF fabricated using RT/Duriod 6010 substrate has a compact size of 7.8 by 26.7 mm. Both the top and the bottom layers of the BPF can be seen from Figure 6(a). The simulated and measured magnitudes of S-parameters are shown in Figure 6(b). Here an excellent agreement is found between simulated and measured results. The measured results show a −3-dB frequency band of 2.6–10.7 GHz. The insertion loss is 0.75 and 1.3 dB at 3.9 and 8 GHz, respectively. The return loss is better than 9 dB in both pass bands of 2.8–5.2 GHz and 5.74–10.8 GHz. Figure 7 shows the simulated and measured S_{21}-magnitudes in 5–6 GHz, where a sharp −3-dB notched band with a maximal attenuation of 21 dB can be observed in the frequency band of 5.2–5.45 GHz. It also can be seen that there is a difference of about 100 MHz between the simulated and measured

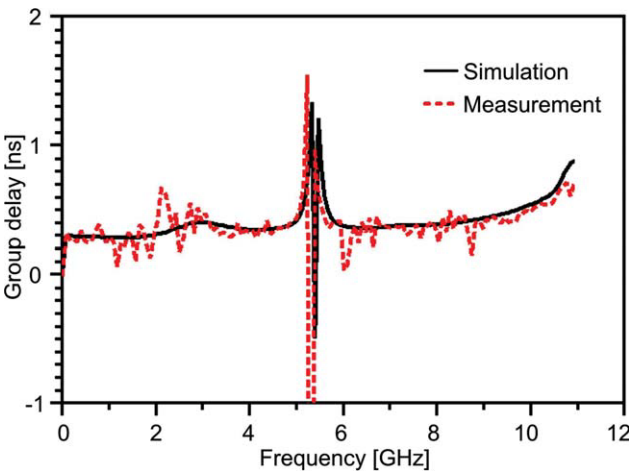

Figure 8 Simulated and measured group delays versus frequency of the UWB BPF. [Color figure can be viewed in the online issue, which is available at www.interscience.wiley.com]

TABLE 1 Comparison of UWB BPFS with Notched Band

Items [Unit]	USB/Atten. [GHz]/[dB]	MSSW [mm]	NBW [%]	MNBR [dB]	Size [mm^2]
[4]	[a]	0.1	6.5[b]	34	22.2 × 15.1
[5]	[a]	0.25	16	22	45 × 14
[6]	[a]	0.08	5.85	20	8 × 6
[7]	11–26/20	0.05	4.6	<10	10.7 × 2.2
[8]	[a]	0.1	1.7	13.8	13.3 × 15
[9]	10–20/23	0.3	22	[a]	25 × 25
This work	12–20/28	0.25	4.7	21	7.8 × 9.4 26.7 × 7.8[c]

USB, upper stop band; MSSW, minimal strip/slot width; MNBR, maximal notched band rejection; NBW, notched band width.
[a] Unknown.
[b] −10 dB.
[c] with LPF section.

notch frequencies. This is attributed to the tolerances in the layout and dielectric constant. When the dielectric constant in the simulation is changed to 10.6 while using the same layout, the simulated S_{21}-magnitude matches the measured result very well (see Fig. 7). The simulated and experimental group delays are shown in Figure 8. The measured group delay varies from 0.4 to 0.7 ns, and 0 to 0.65 ns in the frequency band of 2.6–5.2 GHz and 5.45–10.7 GHz, respectively. It is also clear that the attenuation is more than 28 dB in the upper-stopband from 12 to 20 GHz. Apart from the good in-band performance, a comparison of physical size, minimal strip/slot width, upper stop band attenuation, −3-dB fractional notched bandwidth and maximal notched band rejection between this work and previous work is shown in Table 1. From this comparison it can be seen that this work has the advantage of superior upper stopband attenuation, while providing a rejection of WLAN signal comparable to previous work. This is achieved while maintaining relaxed fabrication constraints and a compact size.

4. CONCLUSION

A compact UWB BPF with a notched band for rejection of in band WLAN signals is presented. The design makes use of a novel rectangular slot ring resonator structure to implement the required WLAN rejection. The novel rectangular slot ring resonator consists of a rectangular slot ring and an S-shaped slot line, and the size of the structure is only 7.8 × 9.4 mm^2 (i.e. 0.46 λ × 0.55 λ, where λ is the guided wavelength of 6.85 GHz). Apart from the good in-band performance shown by measurement results of a prototype filter, the proposed BPF with LPF sections has a compact size of 26.7 × 7.8 mm^2, relaxed fabrication requirement (0.25 mm minimum strip width) and superior attenuation (better than 28 dB from 12 to 20 GHz) in the upper stopband compared with previous work.

ACKNOWLEDGMENT

This work is supported by the Danish Research Council for Technology and Production Sciences under the Grant 274-05-0491.

REFERENCES

1. FCC, Revision of Part 15 of the Commissions Rules Regarding Ultra-Wide-Band Transmission System, ET Docket 98–153, 2002.
2. R. Roovers, D.M.W. Leenaerts, J. Bergervoet, K.S. Harish, R.C.H. van de Beek, G. van der Weide, H. Waite, Y. Zhang, S. Aggarwal, and C. Razzell, An interference-robust receiver for ultra-wideband radio in SiGe BiCMOS technology, IEEE J Solid-State Circuits 40 (2005), 2563–2572.
3. H. Shaman and J. Hong, A novel ultra-wideband (UWB) bandpass filter (BPF) with pairs of transmission zeroes, IEEE Microwave Wireless Compon Lett 17 (2007), 121–123.
4. H. Shaman and J.S. Hong, Ultra-wideband (UWB) bandpass filter with embedded band notch structures, IEEE Microwave Wireless Compon Lett 17 (2007), 193–195.
5. A. Ali and Z. Hu, Metamaterial resonator based wave propagation notch for ultrawideband filter applications, IEEE Antennas Wireless Propag Lett 7 (2008), 210–212.
6. P.-Y. Hsiao and R.-M. Weng, A compact ultra-wideband bandpass filter with WLAN notch band, Microwave Opt Technol Lett 51 (2009), 503–507.
7. S. Wong and L. Zhu, Implementation of compact UWB bandpass filter with a notch-band, IEEE Microwave Wireless Compon Lett 18 (2008), 10–12.
8. S.-S. Gao, S.-Q. Xiao, and B.-Z. Wang, Ultrawideband bandpass filter with a controllable notched band, Microwave Opt Technol Lett 51 (2009), 1745–1748.
9. M.-H. Weng, H. Kuan, W.-L. Chen, C.-S. Ye, and Y.-K. Su, Design of a stopband-improved UWB filter using a pair of shunt and embedded open stubs, Microwave Opt Technol Lett 51 (2009), 2121–2124.
10. K. Gupta, R. Garg, I. Bahl, and P. Bhartia, Microstrip lines and slotlines, Artech House Norwood, Massachusetts, 1996.
11. C. Ho, L. Fan, and K. Chang, Slotline annular ring elements and their applications to resonator, filter and coupler design, IEEE Trans Microwave Theory Tech 41 (1993), 1648–1649.
12. J. Hong and B. Karyamapudi, A general circuit model for defected ground structures in planar transmission lines, IEEE Microwave Wireless Compon Lett 15 (2005), 706–708.

ADDING MICROSTRIP LINE AT THE BOTTOM OF PCB FOR ENHANCING ANTENNA BANDWIDTH

B.-G. Cho, K.-M. Lee, and Y.-S. Kim
Department of Radio Sciences and Engineering, The Graduate School, Korea University, Korea; Corresponding author: bkcho264@korea.ac.kr

Received 4 December 2009

ABSTRACT: *In this article, added microstrip line at the bottom area of printed circuit board (PCB) is proposed for improving the bandwidth of GSM900, DCS1800, and PCS1900. By printing the microstrip line at the bottom area of PCB, frequency bandwidth of slim-type cellular phone which has a low-profile monopole antenna is improved. Dimension of the microstrip line is 45 mm × 9 mm. The width and length of the microstrip line is modified for good bandwidth. The measured return loss of the antenna is better than 7.3 dB for low and high band. Measured peak gains of the proposed antenna present 3.41, 5.48, and 5.95 dBi in each band, respectively. Details of the antenna design are described. Its performances are also presented.* © 2010 Wiley Periodicals, Inc. Microwave Opt Technol Lett 52: 1984–1988, 2010; Published online in Wiley InterScience (www.interscience.wiley.com). DOI 10.1002/mop.25399

Key words: *monopole antenna; mobile antenna*

1. INTRODUCTION

A cellular phone is developed to have a small volume for a good design and to include a lot of parts for multifunctions. This makes the allocated volume of antenna small. A cellular service provider enforces specifications of antenna performance to save a cost and reduce the customer's complains for a bad connection in weak